

Research article

# CHARACTERISTICS OF MADINAT NUGRUS PERALUMINOUS LEUCOGRANITE CARRIER OF RADIOACTIVE MINERALS, SOUTHEASTERN DESERT, EGYPT

Soliman ABU ELATTA Abdallah, Farrage Mohammad KHALEAL & Mohammad  
Abdallah RASHED

Nuclear Materials Authority, P.O. Box. 530, El Maadi, Cairo, Egypt  
E-mail: [dr.soliman72@yahoo.com](mailto:dr.soliman72@yahoo.com)

---

## ABSTRACT

The lithological composition of Madinat Nugrus area in the Southeastern Desert of Egypt comprises a tectonic sequence of dismembered metagabbros, mélange association and mylonites. These rocks are intruded by intracratonic association, which within the mapped area are represented by younger pink biotite granite and peraluminous leucogranite.

Investigation of petrological and mineralogical characteristics of the studied leucogranite indicates that this granite consists of (47% – 52% vol.) sodic plagioclase ( $An_{3-13}$ ), (35% - 40% vol.) quartz, (8% vol.) biotite, (5% vol.) string perthite and (2% vol.) muscovite. Carbonates, garnet, zircon, monazite, apatite, fluorite, metamict uranothorite, columbite, tantalite, sapphire are the common accessories. Alteration products are represented only by soddyite.

Inspection of geochemical characteristics of the studied leucogranite indicates that this granite is monzogranite, peraluminous and sub-alkaline affinities that was emplaced under compressional and tensional regime at relatively shallow depth (water pressure 0.5 - 3 kbar) in the crust and crystallized at temperature range from 700 to 685°C. In general this granite is post Pan-African Orogeny, I-type, originated from highly differentiated magma generated from upper mantle with some contaminations with the crust.

Radiometrical investigation of the studied granite shows uranium contents ranging from 64 to 600 ppm with an average of 218 ppm, thorium contents ranging from 40.5 to 432 ppm with an average of 160 ppm and low Th/U ratio (0.63 – 0.89), suggesting that it is a fertile granite. The main radioactive minerals are metamict uranothorite and soddyite. The very strong positive relationship between U and Th due to the presence of metamict uranothorite as the main radioactive mineral but the poor relationships between U and both of Zr and Rb, in addition to very weak negative relationship between U and Nb indicated that the secondary processes caused the addition of U post magmatically as well as redistribution of U in essential and accessory minerals.

**Key Words:** Nugrus, peraluminous, metamict uranothorite and soddyite.

## 1. INTRODUCTION

The most common peraluminous granites are divided into two groups: the muscovite-bearing peraluminous granites (MPGs) and the cordierite-bearing peraluminous granites (CPGs). The majority of the two groups is produced by partial melting of the crustal rocks. The production of either (MPGs) or (CPGs) does not depend only on the nature of the sources, but is also controlled by the physical parameters of partial melting and consequently by the way anatexis of a thickened crust is enhanced (Barbarin, 1996).

MPGs produced in orogenic zones are affected by major crustal shears or over thrust structures through “wet” anatexis of crustal rocks and crystals fractionation, where they crystallized and exsolved water that may have induced or enhanced water-fluxed melting of the country rock. Nabelek & Main (2004) evaluated thermal models which have previously been proposed for generating leucogranite in collision orogens. CPGs produced through “dry” anatexis of crustal rocks enhanced by underplating or injection of hot mantle – derived magmas (Barbarin, 1996).

World’s economic uranium deposits that are genetically related to granitoids are mostly located in anatectic melts or in strongly peraluminous two mica leucogranites (Poty et al., 1986), in the North American Hercynian Belt (Chatterjee & Strong, 1984), in the Yanshan granitoids of Southeastern China (Jiashu & Zehong, 1984) and in Argentina (Rodrigo & Belluco, 1981).

In Egypt peraluminous leucogranites represent phases of late orogenic to an orogenic granite complex. They brought about Mo, Sn, W, U, and Nb -Ta mineralization in the form of stock works or in the quartz veins within the granitic rocks (Hassan et al., 1984 & Takla et al., 1980).

The present study deals with petrography, geochemistry and mineralization of the mineralized peraluminous leucogranite of Madinat Nugrus, Egypt. An attempt is made to indicate their tectonic environments and throw some light on their mineralogy and its general characteristics.

## 2. GEOLOGICAL SETTING

The mapped area of Madinat Nugrus is located in the Southeastern Desert 75 km southwest of coastal Marsa Alam City on the Red Sea, between Lon. 34° 45' 45" - 34° 46' 15" E and Lat. 24° 37' 15" - 24° 37' 45" N (Fig. 1). The basement rocks in this area are arranged according to their increasing age as follows: metagabbros, ophiolitic mélange, mylonites, pink biotite granites and peraluminous leucogranite (two micas granite).

### 2.1. Metagabbros

Metagabbros are the oldest stratigraphic member, occurring southeast of the study area. These metagabbros are member of ophiolitic sequence of Wadi Ghadir-Sikait fold belt and are thrust over ophiolitic mélange from the west (Fig. 1). The thrusting angle changes as a result of the intrusion of the peraluminous leucogranite in ophiolitic mélange. In the northwest and southwest metagabbros are cut and bounded by Wadi Abu Rushied and Nugrus, respectively, while in the southeast they extend beyond the limits of the study area.

Metagabbros are dissected by NE-SW trending dextral and NNE-SSW trending sinistral strike-slip faults as well as NW-SE trending normal fault (Figs. 1 & 2a) and some pegmatite dykes and quartz veins. Metagabbros are characterized by pockets of pegmatitic gabbros rich in feldspars, some of which are pink in color, anorthosites and trondhjemite. These represent injections of the late stage differentiates of the gabbroic magma. They are cut by quartz veins, showing gneissose texture and composed mainly of plagioclase, hornblende and clinopyroxene. Apatite, biotite and opaques are accessories while chlorite is the alteration product.

### 2.2. Ophiolitic mélange

Ophiolitic mélange in the study area occurs as intermixed zone of pervasively deformed matrix of metasedimentary origin intermingled with fragments of serpentinites, metapyroxenites, metagabbros, metadiabase and metabasalts varying in size, thus forming the olistostrome type.

These rocks are thrust over mylonite rocks and intruded by peraluminous leucogranite from northeast. The most of foliation strikes of ophiolitic *mélange* are parallel to the strike of the thrust fault which affected the ophiolitic *mélange*. Many drag folds were developed along the thrust in both mylonites and ophiolitic *mélange* (Fig. 2b). These drag folds were symmetric or asymmetric open anticlines at first stage of thrusting and became angular overturned and chevron recumbent folds as the thrusting progressed. The thrust fault was reactivated as left strike slip fault, perhaps at the end of Pan African orogeny, with developed S- shape drag folds along its plane in ophiolitic *mélange* (Fig. 2c). Also these rocks are cut by Wadi Abu Rushied in the northwest and in the southeast they extend beyond the limits of the study area. Rocks of ophiolitic *mélange* are dissected by dextral NE-SW trending and sinistral NNE-SSW trending strike-slip faults as well as NW-SE trending normal fault and some pegmatite dykes and quartz veins.

The fine to medium-grained metasedimentary matrix is represented by meta-calc-pelites (para-amphibolites and hornblende biotite schists) and meta-psammopelites (banded muscovite biotite schist and quartzofeldspathic biotite schist, Saleh, 1997). They are composed mainly of quartz, plagioclase, tremolite-actinolite and biotite. Muscovite, apatite, chlorite, zircon and garnet are secondary and accessory minerals.

### 2.3. Mylonitic rocks

Mylonites in the study area have a crescent shape. They are intruded by pink biotite granites in the east, while in the north and south they extend beyond the limit of the study area and in the west they are bounded by thrust of ophiolitic *mélange* and intruded peraluminous leucogranite. The mylonitic rocks contain quartz veins resulting from extensive recrystallization and remobilization of quartz. The mylonites are cut by NNE-SSW, ENE-WSW and N-S trending sinistral strike-slip faults and NE-SW and NNW-SSE trending dextral strike-slip faults.

The main alteration processes in mylonites are hematitization, greisenization, silification, albitization, fluoritization and pyritization as a result of hydrothermal solutions passing up through cracks induced by strike slip faults. Mylonites are fine to medium grained; composed mainly of quartz, alkali feldspars, plagioclase (An<sub>7-15</sub>), and biotite, together with zircon, apatite, allanite, titanite and opaques.

### 2.4. Pink biotite granites

Pink biotite granites occur in the eastern part of the study area and extend beyond its limit except on the western side where they intrude mylonites. Morphologically, these rocks are high rugged mountain peaks and highly joints as a result of their cut by NE-SW and NNW-SSE trending dextral strike-slip faults and ENE-WSW and N-S trending sinistral strike-slip faults. Many of alterations occur along the faults and joints. Pink biotite granites are composed mainly of subhedral to anhedral quartz crystals, subhedral to euhedral cracked plagioclase crystals, K- feldspars (orthoclase, micro-perthite and microcline) and elongated shreds or thin flakes of biotite crystals. The accessories are zircon, opaques and apatite.

### 2.5. Peraluminous leucogranite (two micas granite)

The peraluminous leucogranite in the mapped area occurs as a curved dyke like body along the contact of ophiolitic *mélange* with mylonites. It may represent a tongue of sub- hidden body formed along the major strike slip fault running in the NW-SSE direction. The dyke like body (Fig. 2d) formed along one branch of NNW-SSE strike slip fault cut by NE – SW trending dextral strike slip faults and NNE – SSW and NW – SE trending sinistral strike slip faults. In some of its parts, peraluminous leucogranite is pegmatitic, contains coarse grained muscovite and xenoliths of mafic rocks as well as black mica pockets and crystals of garnets. Microscopically, they are composed mainly of (47% - 52 % vol.) euhedral to subhedral sodic plagioclase (An<sub>3-13</sub>), (35% - 40% vol.) quartz, (8% by vol.) biotite (Fig. 3a), as well as euhedral to subhedral string perthite (5% vol.) and muscovite (2 vol. %) (Fig. 3b). Carbonate, garnet, metamict uranotorite, zircon (Fig. 3c), monazite, apatite, fluorite (rose and colorless) and opaques are the common accessories. Alteration products are represented only by a secondary uranium mineral (soddyite as indicated by ESEM) and carbonate (Fig. 3d). The presence of garnet, primary muscovite flakes and corundum (as mineral and normative) reflects the peraluminous nature.

### 3. MATERIALS AND METHODS

#### 3.1. Field work

The field work included identification, description and mapping of different exposed rock units. Radiometrical measurements of different rock units with emphasis on the peraluminous leucogranite were carried out on foot using a portable gamma-gun spectrometer (Fd-3013 mode, made in China). Twelve samples of the peraluminous leucogranite from Madinat Nugrus were collected for different purposes.

#### 3.2. Laboratory methods

The petrographical studies were carried out on twelve thin sections of the peraluminous leucogranite using a Nikon (optical – pol) polarizing microscope equipped with a full automatic microphotograph attachment (Microflex AFX – II).

A total of nine representative samples with size 200 mesh were chosen from the peraluminous leucogranite for chemical analysis in the laboratories of the Nuclear Materials Authority (N M A). The major oxides were determined by wet chemical technique (Shapiro and Brannock, 1962). The significant trace elements were determined by X – ray fluorescence method (Philips – PW 1480 X – ray) spectrometer X unique II with automatic sample changer ( PW – 1510 ). The uranium and thorium contents were measured chemically through Arzenazo (III). The results of chemical analyses are presented in Table 1, together with the calculated CIPW norm.

Mineralogical investigation of the heavy minerals was carried out by using X – ray diffraction (XRD) and environmental scanning electron microscopy coupled with energy dispersive spectroscopy ESEM/EDX to identify different minerals.

### 4. RESULTS AND DISCUSSION

#### 4. 1. MINERALOGY OF PERALUMINOUS LEUCOGRANITE

Results of detailed mineralogical studies of peraluminous leucogranite are presented in the following paragraphs.

##### 4.1.1. Uranium and thorium minerals

Uranium and thorium minerals in this rock are represented by soddyite  $(\text{UO}_2)_2 \text{SiO}_4 \cdot 2\text{H}_2\text{O}$  and uranothorite  $(\text{Th, U}) \text{SiO}_4$ .

##### *Soddyite $(\text{UO}_2)_2 \text{SiO}_4 \cdot 2\text{H}_2\text{O}$*

Soddyite occurs in this rock as yellow patches (Fig. 4a) and contains 45% U, 22% Si and many impurities of Fe (13%), Nb (8%), Ca (5%), K (3.5%), and Na (2.5%) in decreasing order as indicated by semi quantitative chemical analysis using ESEM/EDX (Fig. 4a), this mineral is formed in carbonate crystals or on the surfaces of other crystals due to the post magmatic processes, which influenced the primary ones.

##### *Uraniothorite $(\text{Th, U}) \text{SiO}_4$*

Uraniothorite is metamict and occurs in this rock in four morphological varieties, 1-yellowish brown metamict prismatic crystals (Figs. 4b & 5a) terminated by di- pyramids, 2-yellowish brown metamict grains coated with carbonate (Figs. 4c, d & 5b), 3- brown grains on the surface of almandine garnet (Figs. 4e & f) and 4- assemblage crystals of uranothorite, columbite and zircon or uranothorite and tantalite.

The first morphological variety (Fig. 4b) contains 23% U, 64% Th and 10.47% Si as well as 2 % Ca as impurity. The second variety (Fig. 4c) contains 14.5% U, 59.3% Th, and 12% Si. The third variety contains 61% Th, 16.5% U and 12% Si as indicated by semi quantitative chemical analysis ESEM/EDX (Fig. 4e). The fourth variety, assemblage crystals of uranothorite, columbite and zircon or uranothorite and tantalite was identified by XRD (Figs. 5c & d).

#### 4.1.2. Niobium – tantalum minerals

Niobium and tantalum minerals are represented by columbite and tantalite.

##### *Columbite (Fe, Mn) (Nb, Ta)<sub>2</sub>O<sub>6</sub>*

Columbite occurs in this rock as rare black prisms (up to 5mm in size) and showing submetallic to subresinous luster. The examined prisms by XRD show, they are assemblage crystals of columbite, uranothorite and zircon (Fig. 5c) but semi-quantitative chemical analysis using ESEM/EDX for the columbite minerals Fig. 6a) indicated that, they contain many elements such as Ca, Al, Mg, Na, U, Ce, Y and Ti as impurities, also indicated a decrease Fe and the Nb/Ta ratio from core to margin and an increase in Ce and Al (Table 2). Also Y and U slightly increased from core to margin (Table 2). This reflects relation between the Nb/Ta ratio and these elements during crystallization.

##### *Tantalite (Fe, Mn) (Ta, Nb)<sub>2</sub>O<sub>6</sub>*

Tantalite occurs as rare brown prisms. These crystals were examined by ESEM/EDX which contains 45% Ta, 27% Nb, 7.5% Mn (Fig. 6b) and many other elements, such as Ca (4.63%), Al (2.3%), Na (1.3%), HREE (Yb) (5%), Y (4%) and Ti (1.5%) as impurities. Tantalite was also found in assemblage crystals together with uranothorite as indicated by XRD analysis (Fig. 5d).

#### 4.1.3. Hafnian zircon (Zr, Hf) SiO<sub>4</sub>

Hafnian zircon in the studied peraluminous leucogranite occurs as prismatic to dipyramidal crystals which are frequently twinned. It is usually of brown, green and blue colors. This mineral was identified by XRD (Fig. 5c) and ESEM/EDX. (Fig. 5c) According to ESEM/EDX analysis it contains 27.34 % Si, 57.91 % Zr and 7% Hf and was thus designated as a hafnian zircon according to Correia Neves et al. (1974). It also contains some impurities of U (1.3%), Al (2.79%), Fe (1.37%) and Na (1.89%). The occurrence of U in zircon crystals indicates the strong final effects of hydrothermal fluids on these crystals and may also indicate differential expulsion of cations from zircon under hydrothermal fluids (Hoskin & Schaltegger, 2003).

Irber (1999) indicated that the Zr/Hf ratios for peraluminous granites of mideastern Germany varying among (9 – 39) with lower ratios (<20) are affected by strong magmatic hydrothermal alterations. The Zr/Hf ratio in common granites is about 39 (Erlank et al., 1978) and are mostly close to the chondritic ratio of 38 (Anders & Grevesse, 1989). Zircon crystals in the studied rock show the Zr/Hf ratio 8.27, which indicates they were subjected to strong hydrothermal alteration.

#### 4.1.4. Native bismuth

Bismuth occurs in the study area in peraluminous leucogranite as reddish brown grains with strong metallic luster. It also forms, slightly malleable, highly fractured granular aggregates and plumose dendrites. Bismuth was identified by ESEM/EDX (Fig. 6d) and contains 93% Bi as well as minor Si, Al and Mg.

#### 4.1.5 Sapphire (Al<sub>2</sub>O<sub>3</sub>)

In the studied rocks, sapphire occurs as blue tabular crystals found along the margin of peraluminous leucogranite, the blue color may be due to Ti (Heinrich, 1959). This mineral was identified by ESEM/EDX (Fig. 6e) contains 65 % Al as well as 11%Si, 13.5%S and 6.7%Cl as impurities. The occurrence Cl indicates

action of pneumatolytic agents upon alumina – bearing schist of ophiolitic mélange and peraluminous leucogranite play very important role in sapphire formation (Heinrich, 1959).

#### 4.1.6. Fluorite (CaF<sub>2</sub>)

The fluorite is composed mainly of Ca and F and occasionally contains many other impurities such as Cl, Fe, REE, in rare instances also U and helium (Heinrich, 1959). Fluorites crystallize in cubic system and occur as colorless or yellow, green blue, violet and violet black colors. The coloration is caused by the appearance of electrically neutral of Ca and F atoms in the crystal structure (Heinrich, 1959). Fluorite in studied the peraluminous leucogranite occurs as violet and colorless crystals. This mineral was identified by petrographic description and ESEM/EDX (Fig. 6f). It contains 65% Ca and 26% F and some impurities of Si and Al.

#### 4.1.7. Almandine garnet (Fe<sup>2+</sup><sub>3</sub>Al<sub>2</sub>(SiO<sub>4</sub>)<sub>3</sub>)

Almandine garnet occurs as reddish brown trapezohedron crystals with vitreous luster. This mineral is often significant for the peraluminous rocks. Almandine garnet was identified by petrographic description and ESEM/EDX (Figs. 4f & 6g). It contains 14% Fe, 20% Al and 52% Si as well as impurities of Mg (7.5%), Ca (3%), K (2.5%) and Ti (1.5%).

### 4.2 Geochemical features of peraluminous leucogranite

The results of the chemical analysis of peraluminous leucogranite depend on the behavior and distribution of major and trace elements in the rocks. The comparison of average chemical composition of the studied granitic rock with Group II younger granites of Eastern Desert of Egypt (Greenberg, 1981) showed that they have the same value of SiO<sub>2</sub>, nearly the same Al<sub>2</sub>O<sub>3</sub> and TiO<sub>2</sub> and higher MgO, CaO, Na<sub>2</sub>O and P<sub>2</sub>O<sub>5</sub> and lower K<sub>2</sub>O. Compared to group III they have higher SiO<sub>2</sub>, Na<sub>2</sub>O and P<sub>2</sub>O<sub>5</sub> and lower TiO<sub>2</sub>, Fe<sub>2</sub>O<sub>3</sub>, MgO, CaO and K<sub>2</sub>O. When compared with two micas granite of G. El Sella (Ibrahim et al., 2003) they have higher in SiO<sub>2</sub>, Al<sub>2</sub>O<sub>3</sub> and P<sub>2</sub>O<sub>5</sub> and lower in Fe<sub>2</sub>O<sub>3</sub>, MgO, CaO and K<sub>2</sub>O. The average chemical composition of the studied granitic rock shows that, when compared with an average of the World granites (Le maitre, 1976), they have higher SiO<sub>2</sub>, Fe<sub>2</sub>O<sub>3</sub>, P<sub>2</sub>O<sub>5</sub> and Na<sub>2</sub>O and lower Al<sub>2</sub>O<sub>3</sub>, MgO, CaO, and K<sub>2</sub>O. When compared with the average chemical composition of the studied granitic rocks of Egyptian granites (Aly & Moustafa, 1984), they show an increase in SiO<sub>2</sub>, Fe<sub>2</sub>O<sub>3</sub>, P<sub>2</sub>O<sub>5</sub> and Na<sub>2</sub>O, a decrease in K<sub>2</sub>O, slight decrease in Al<sub>2</sub>O<sub>3</sub> and MgO and the same value in TiO<sub>2</sub> as shown in Table 3.

### 4.3. Geochemical classification, magma type, temperature formation and tectonic setting

According to the normative classification diagram (Fig. 7), the samples of the studied rock mostly fall in the monzogranite field. They are sub-alkaline (Fig. 8) and have peraluminous character (Fig. 9). On the Na<sub>2</sub>O – K<sub>2</sub>O diagram (Fig.10), they are I- type granites that were subjected to Na-metasomatism (Fig.11) during crystal fractionation by the hydrotherms. They plot near to the ternary minima in the normative Q-Ab-Or diagram at 0.5 - 3 kbar P<sub>H<sub>2</sub>O</sub> (Fig.12), suggesting that it crystallized at relatively shallow depths. In general, the studied rock crystallized in temperature range from 685 to 700°C (Fig. 13). This result is supported by the zirconium concentrations in the studied peraluminous leucogranite which are below 100 ppm in all samples, as the higher concentrations of Zr in the granites (> 100 ppm) indicate that they formed at temperature higher than 800°C (Watson & Harrison, 1983). According to the Nb – Y and SiO<sub>2</sub>–Al<sub>2</sub>O<sub>3</sub> diagrams (Figs. 14 & 15), the studied granites are within – plate, post orogeny respectively and were emplaced in an interference area between compressional and tensional regimes according to AFM diagram (Fig. 16).

### 4.4. Petrogenetic implications

The differentiation index (D.I. = Q + Or + Ab; Thornton & Tuttle, 1960) values of the granite are generally high (89.28-91.76) (Table 1) and indicate highly differentiated magma. Moreover Cox et al. (1979) indicated that Na<sub>2</sub>O/K<sub>2</sub>O ratio is less than one in the granitoids of crustal origin but the studied granite shows a higher average Na<sub>2</sub>O / K<sub>2</sub>O ratio, which is 5.4. This suggests mantle origin. It is well known that, The K/ Rb ratio is used as differentiation index, where it decreases with the increasing magmatic fractionation. This ratio in the

igneous rocks derived mainly from upper mantle materials, ranges from 700 – 1500 (Heier, 1973), while Madinat Nugrus peraluminous granite shows that K/Rb ratios range from 78.45-114.77 and the K/ Ba ratios range from 436.83 to 700 (Table 1) as well as the K/Rb-Rb diagram (Fig. 17) which shows the plotting samples have the same trend, may be attributed to this granite formed from advanced differentiation one magma as well as contribution of sialic crustal material.

It is well known that the average Ba/Rb ratio of the crust is 4.4 (Shaw, 1968). However the Ba -Rb variation diagram (Fig. 18) indicates the peraluminous granite samples scatter between Ba/Rb ratios of 0.044 and 0.44, in addition, these rock are depleted in Ba relative to Rb probably due to advanced differentiation of the feldspars crystallization as well as mantle origin for these rocks.

#### 4. 5. RADIOACTIVITY

The radioactivity of the studied peraluminous leucogranite appears higher than of the surrounding rocks. Thus the radioactivity of the granite ranges from 400 to 3000 cps while the radioactivity of other adjacent rocks (especially mylonites) does not exceed 800 cps. Also we found that radioactivity measurements frequently exceeded 800 cps in the peraluminous leucogranite (two micas granite).

#### 4.6. Geochemistry of uranium and thorium

Uranium has two common oxidation states (+ 4 and + 6) resulting in distinctly different geochemical behavior and affinity under different redox conditions. Thorium has only one common oxidation state (+ 4) and is usually found as a trace element in most mineral phases.  $U^{4+}$  and  $Th^{4+}$  have similar chemical properties (e.g. ionic charge, effective radius, and coordination number) (Shannon, 1976) at the magmatic thorium occur as  $U^{+4}$  and  $Th^{+4}$ ,  $U^{+4}$  can substitute for  $Ca^{+2}$  in a few minerals such as apatite and sphene as the crystallization of the magma proceeds, U and Th tend to concentrate in the residual fluids until they compete with those elements for which they can substitute or form minerals of their own.

In general, during magmatic differentiation U and Th content increase from basaltic to low Ca-granitic rocks. However, low Ca-granites may be enriched in Th relative to U because some U enters into an aqueous phase as uranyl ions during the final stages of crystallization of granitic magmas (Bowen & Attendorn, 1988). On the surface and under highly oxidizing conditions,  $U^{+6}$  is the dominant stable form while thorium occurs as  $Th^{+4}$ .

#### 4.7. Distribution and behavior of uranium and thorium in peraluminous leucogranite

Studied rocks have U and Th contents ranging from 64 to 600 ppm and from 40.5 to 432 ppm with an average of 218 and 160 ppm respectively. They show high U and Th concentrations that could be related to acidic igneous rocks (U = 1-12 ppm) and (Th = 5-20 ppm) of IAEA (1979) and Boyl (1982). The average U content in Madinat Nugrus granite is more than twice of Clarke value (4ppm), which supports the assumption that the studied granite is considered as fertile granite.

U, Th, Zr, Nb and Rb behave compatibly in granitic melt, so that where U concentration is controlled by magmatic processes, these elements would be expected to increase (Briqueu, 1984). In the work, the plot of U against Th (Fig. 19a ) shows strong positive correlation presumably due to the presence of metamict uranothorite mineral as the principal radioactive mineral, while plots of U against Zr, Rb, and Nb (Figs.19b, c & d) show poor or very weak negative correlations, suggesting, addition of U in the post magmatic processes. The crustal average of the Th/U ratio is 3.8 (Taylor and McLennan, 1985), when this ratio is disturbed; it indicates addition or removal of U since Th is relatively stable during post magmatic processes. The Th/U ratio in the studied granite ranges from 0.68 - 0.89, suggesting post magmatic addition of U.

### 5. CONCLUSION

- 1- The tectonostratigraphic sequence of the rocks at Madinat Nugrus can be arranged according to their increasing age as follows: metagabbros, ophiolitic mélange, mylonites, pink biotite granites and peraluminous leucogranite (two micas granite).

- 2- Madinat Nugrus peraluminous leucogranite (two micas granite) was formed along the NW-SE strike slip fault curved to NNW-SSE as a result of rising magma from upper mantle in this weakened zone, which is a branch of Nugrus major strike slip fault that formed along the previous Nugrus thrust during extensional collapse after post Pan African tectonics.
- 3- The petrographical and mineralogical studies revealed that this granite is composed of (47 – 52% vol.) sodic plagioclase ( $An_{3-13}$ ), (35 - 40% vol.), Quartz, ( 8% vol.) biotite, ( 5% vol.) string perthite and (2% vol.) muscovite. Carbonate, garnet, zircon, monazite, apatite, fluorite (rose and colorless), metamict uranothorite, columbite, tantalite, sapphire are the common accessories. Alteration products are represented only by secondary uranium mineral soddyite as indicated by ESEM/EDX.
- 4- Madinat Nugrus leucogranite (two micas granite) is classified according to geochemical studies as monzogranite, peraluminous and sub- alkaline affinities, emplaced under compressional and tensional regime at relatively shallow depth (water pressure 0.5- 3 kbar) in the crust and crystallized at temperature range from 700 to 685°C. In general this granite is within plate; post Pan- African orogeny, I-type, originated highly differentiated magma generated from upper mantle with some contaminations with the crust.
- 5- Studies of radioactivity revealed that, this granite is a fertile type in places where:
  - a- It is peraluminous (presence of primary muscovite, almandine garnet, sapphire and normative corundum).
  - b- It is highly differentiated (depleted in Sr, Ba and relatively high Rb).
  - c- The Th/U ratios are very low (0.63 – 0.89) compared to the ratio of normal granitic rocks, which is 3.8.
  - d- The uranium contents range from 64- 600 ppm (with an average 218 ppm), while the thorium contents range from (40.5 to 432 ppm with an average of 160 ppm).

The very strong positive relationship between U and Th due to the presence of metamict uranothorite as the main radioactive mineral but the poor relationships between U and both of Zr and Rb , in addition to very weak negative relationship between U and Nb suggested that the secondary processes caused the addition of U post magmatically as well as redistribution of U in essential and accessory minerals. Only soddyite was recorded as secondary uranium mineral otherwise uranium is mainly concentrated in metamict uranothorite as well as in some minerals as columbite, tantalite and hematite.

## REFERENCES

- [1] Aly, M. M. & Moustafa, M. M. 1984: Major chemistry statistics characterizing common igneous rocks of Egypt. 9<sup>th</sup> Inter. Cong. Stat. Comp. Sci. Res., Ain Shams University, Cairo, Egypt.
- [2] Anders, E. & Grevesse, N. 1989: Abundance of the elements: Meteoritic and solar. *Geochimica et Cosmochimica Acta*, 53: 197-214.
- [3] Barbarin, B. 1996: Genesis of the two main types of peraluminous granitoids. *Geological Journal*, 24, no. 4: 295 – 298.
- [4] Bowen, R. & Attendorn, H. G. 1988: *Isotope in the earth sciences* (1st Edition), Springer, 531P
- [5] Boyl, R. W. 1982: *Geochemical prospecting for thorium and uranium deposits*. Elsevier: Amsterdam and New York, 498p.
- [6] Briquieu, L., Bougaut, H. & Joron, J. L. 1984: Quantification of Nb, Ta, Ti, V, anomalies in magmas associated with subduction zones: Petrogenetic implications, *Earth and Planetary Sciences*, 68: 279-308.
- [7] Chatterjee, A. K. & Strong, D. F. 1984: Discriminate and factor analysis of geochemical data from granitoid rocks hosting the Millet Brook uranium mineralization, South Mountain Batholith, Nova Scotia, *Uranium*, 1: 289 – 305.
- [8] Correia Neves, J.M., Lopes Nunes J.E. & Sahama, Th. G. 1974: High hafnium members of zircon-hafnion series from the granites pegmatite of Zambezia, Mozambique. *Contribution to Mineralogy & Petrology*, 48: 73-80.
- [9] Cox, K. G. Bell, j. d. & Pankhurst, R. J. 1979: *The interpretation of igneous rocks*. William Clowes, London, Britain, 414 p.

- [10] **Cuney, M., Leroy, J., Volivezo, A., Daziano, C., Gambola, B., Zarco, A. J., Morello, O., Ninci, C. & Molina, P. 1989:** Geochemistry of the uranium mineralized Achala granitic complex, Argentina: comparison with Hercynian peraluminous leucogranites of Western Europe. *Procedures Technical Committee Meetings, Vienna, Tecdoc-543, I AE A, Vienna, 211-232.*
- [11] **Erlank, A. J., Marchant, J. W., Cardoso, M. P. & Ahrens, L. H. 1978:** Zirconium. In *Handbook of geochemistry*(ed. K. H. Wedepohl). B-O. Springer, Part II, 4, 40p.
- [12] **Greenberg, J. K.; 1981:** Characteristic and origin of Egyptian youngest granites. *Summary, Bulletin Geological Society of America, Part II, 92: 749 – 840.*
- [13] **Hassan, M., El-Bakry, H., Al-Amin, & Al Bassiony, Q. 1984:** Geochemical orientation survey of tungsten mineralization in arid conditions, eastern desert, Egypt. *Bulletin Faculty of Science Zagazig University, 6: 38-54.*
- [14] **Heier, K. S. 1973:** Geochemistry of granulite facies rocks and problems of their origin. *Philos. Trans. Roy. Soc. London, Series, 273: 429-442.*
- [15] **Heinrich, E. W. 1959:** *Geology of radioactive raw materials.* Mc Graw-Hill, New York, 654p
- [16] **Hoskin, P.O. and Schaltegger, U. 2003:** The composition of zircon and igneous and metamorphic petrogenesis: in Hanchar, *Journal of Mineralogy and Hoskin, P.W.O., eds.*
- [17] **(IAEA) International Atomic Energy, Agency, 1979:** Gamma ray surveys in uranium exploration, *Technical Report. Vienna, Series, paper no. 186, 90 p.*
- [18] **Ibrahim, M. A., Zalata, A. A., Assaf, H. S., Ibrahim, I. H. & Rashed, M. A. 2003:** El Sella shearing zone, Southeastern Desert: An example of vein-type uranium deposit. *The 9<sup>th</sup> International Mining, Petroleum and Metallurgical Engineering Conference, Cairo University, 1 – 17.*
- [19] **Irber, W. 1999:** The lanthanide tetrad effect and its correlation with K/ Rb, Eu/ Eu\*, Sr/ Eu, Y/ Ho and Zr/ Hf of evolving peraluminous granite suites. *Geochimica et Cosmochimica Acta, 63: 489-508.*
- [20] **Irvine, T. N. & Baragar, W. R. A. 1971:** A guide to the chemical classification of the common volcanic rocks, *Canadian Journal of Earth Science, 8: 523-548.*
- [21] **Jiashu, R. & Zehong, H. 1984:** Form of uranium occurrence and its distribution in uraniferous granites, In: *Geology of granites and their Metallogenetic Relations, Proc. Symp. Nonjing, University Press, Beijing, 621 – 635.*
- [22] **Le Maitre, R. W. 1976:** The chemical variability of some common igneous rocks. *Journal of Petrology, 17: 589 – 637.*
- [23] **Maniar, P.D. & Piccoli, P. M. 1989:** Tectonic discrimination of granitoids. *Bulletin Geological Society of America, 101: 635-643*
- [24] **Nabelek, P. I. & Mian, L. 2004:** Petrologic and thermal constraints on the origin of leucogranites in collisional orogens. *Transactions of the Royal Society of Edinburgh: Earth Sciences, 95: 73-85.*
- [25] **Pearce, J. A.; Harris, N. B. W & Tindle, A. G. 1984:** Trace element discrimination diagrams for the tectonic interpretation of granitic rocks. *Journal of Petrology, 25: 958-983.*
- [26] **Petro, W.L., Vogel, T.A. & Wilband, J.T. 1979:** Major elements chemistry of plutonic rock suites from compressional and extensional plate boundaries, *Chemical Geology, 26: 217-235.*
- [27] **Poty, B., Leory, J., Cathelineau, M., Cuney, M., Friedrich, M., Lespinassa, M. & Turpin, L. 1986:** Uranium deposits spatially related to granites in the French part of the Hercynian orogen, In: *Vein type uranium deposits, I. A. E. A., Vienna, Tecdoc, 361: 215 – 246.*
- [28] **Rodrigo, F. & Belluco, A. E. 1981:** Programa nacional de desarrollo de los recursos uraniferos de la Argentina, In: *uranium deposits in Latin America: Geology and Exploration, IAEA, Vienna, 395 – 414.*
- [29] **Saleh, G.M. 1997:** The potentiality of uranium occurrences in Wadi Nugrus area, South Eastern Desert, Egypt. *Ph. D. Thesis, Faculty of science, Mansoura University, 171p.*
- [30] **Shand, S. J. 1951:** *The study of rocks: Murby, London, 236p.*
- [31] **Shannon, R. D. 1976:** Revised effective ionic radii and systematic studies of interatomic distances in halides and chalcogenides. *Acta Crystallographica Section A: Foundations of Crystallography A32: 751 – 767.*
- [32] **Shapiro, L., and Brannock, W. W., 1962:** Rapid analysis of silicate, carbonate and phosphate rocks. *U.S. Geological Survey, Bull, V. 114A, 56p.*
- [33] **Shaw, D. M. 1968:** A review of K/Rb fractionation trends by covariance analysis. *Geochimica et Cosmochimica Acta, 32: 573-601.*
- [34] **Streckeisen, A. 1976:** Classification of the common igneous rocks by means of their chemical composition. *Aprovisional attempt. Neues Jahrbuch für Mineralogie – Monatshefte, 1-15.*

- [35] Takla, M. A. & Noweir, A. M. 1980: Mineralogy and mineral chemistry of the ultramafic mass of El-Rubshi, Eastern Desert, Egypt. Neues Jahrbuch für Mineralogie - Abhandlungen. Stuttgart: 140 (1), 17 - 28.
- [36] Taylor, S. R. & McClelland, S. M. 1985: The Continental Crust: Its Composition and Evolution. Blackwell Scientific Publications, Oxford, 1985.
- [37] Thornton, C. P. & Tuttle, O. F. 1960: Chemistry of igneous rocks. Differentiation index. American Journal of Science, 258, 664-684.
- [38] Tuttle, O. F. & Bowen, N. L. 1958: Origin of granite in the light of experimental studies in the system  $\text{NaAlSi}_3\text{O}_8\text{-KAlSi}_3\text{O}_8\text{-SiO}_2\text{-H}_2\text{O}$ , Geological Society America Memoir, 74:1- 153.
- [39] Watson E. & Harrison, T. M. 1983: Zircon saturation revisited: temperature and composition effects in a variety of crustal magma types. Earth and Planetary Science, 64: 295 – 304.
- [40] White, A. J. R. & Chappell, B. W. 1984: Granitoid types and their distribution in the Lachlan Fold Belt. South Eastern Australia, Geological Society America Memoir, 159: 21-34.

**Figures:**

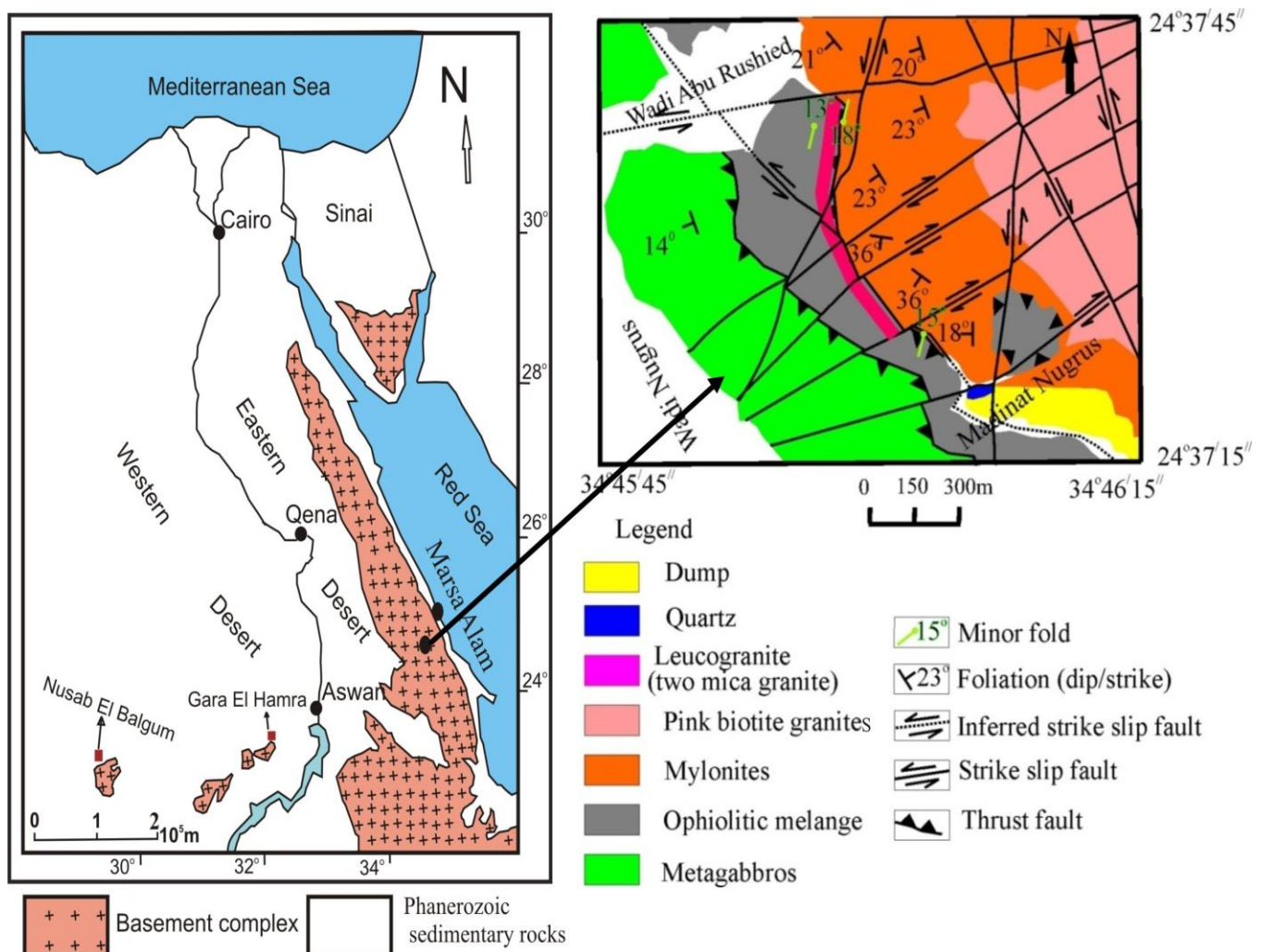


**Figure1:** Location and geological map of the study area.

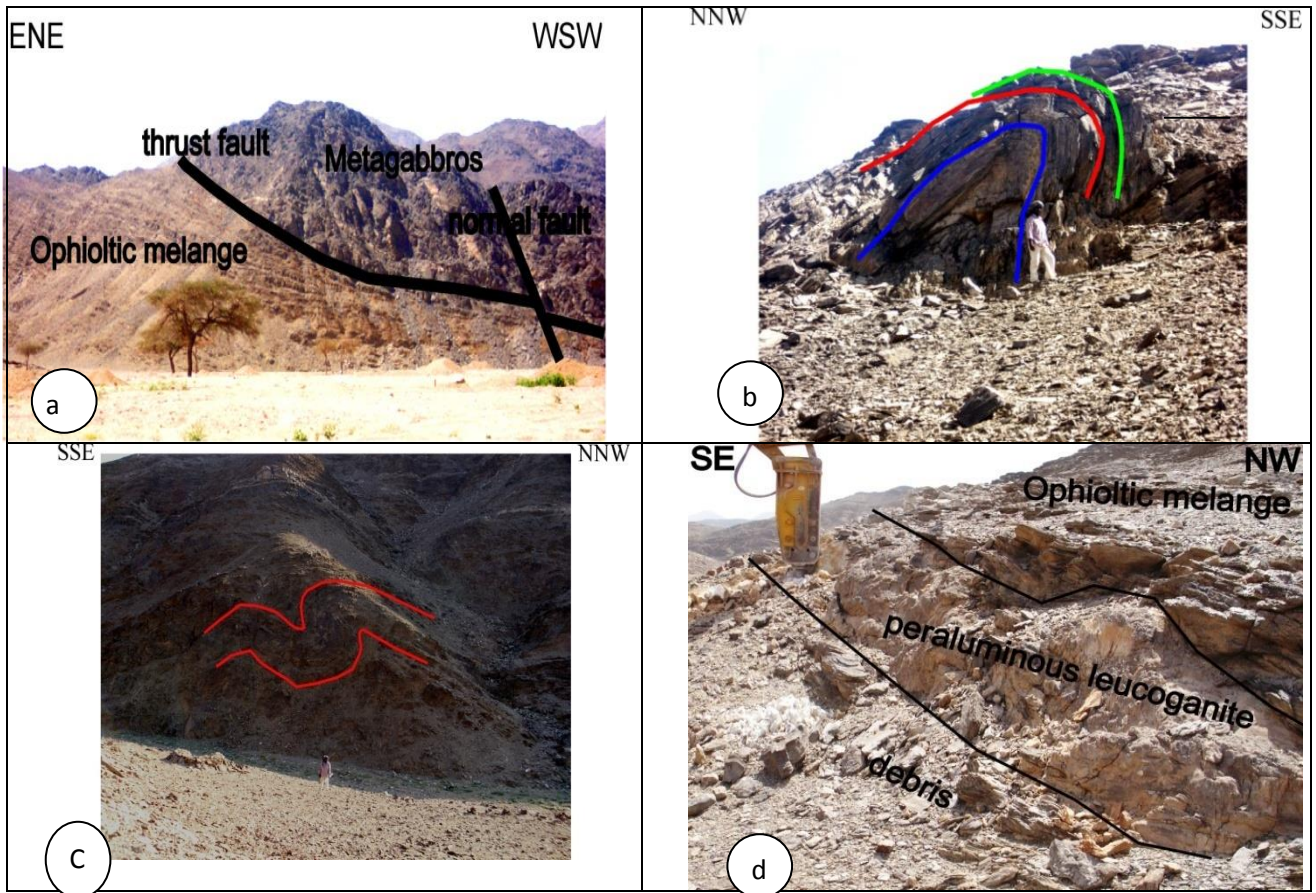


**Figure 2:** Field photographs showing: a. thrust metagabbros over ophiolitic mélange and normal fault, b. drag chevron fold in ophiolitic mélange along thrust, c. s-shape fold along the plane of left strike slip fault and d. dyke like body of leucogranite.

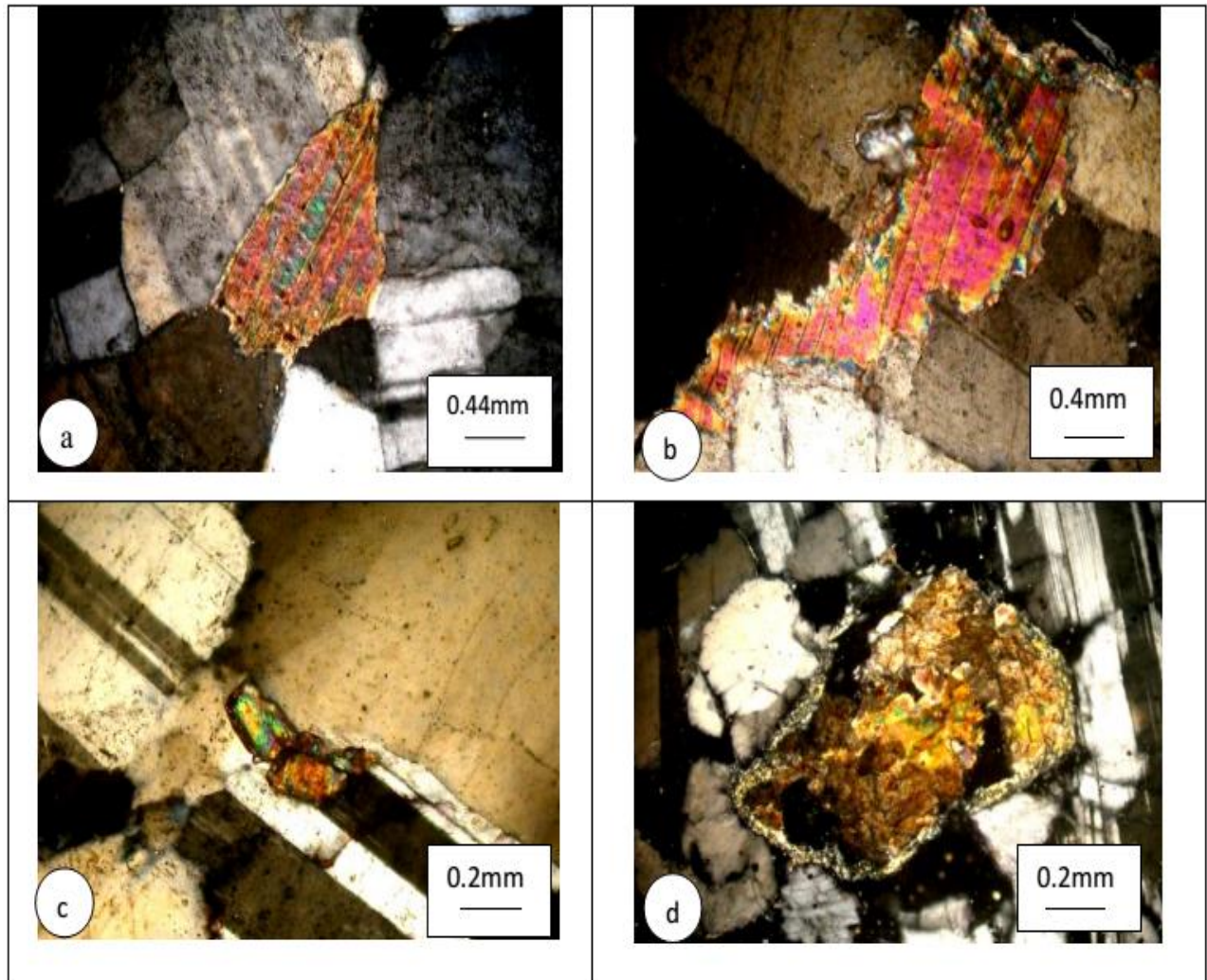


**Figure 3:** Optical microphotographs (R.L.) showing: a. biotite, b. muscovite, c. zircon and d. secondary uranium (soddyite) in leucogranite. R.L. = reflected light.

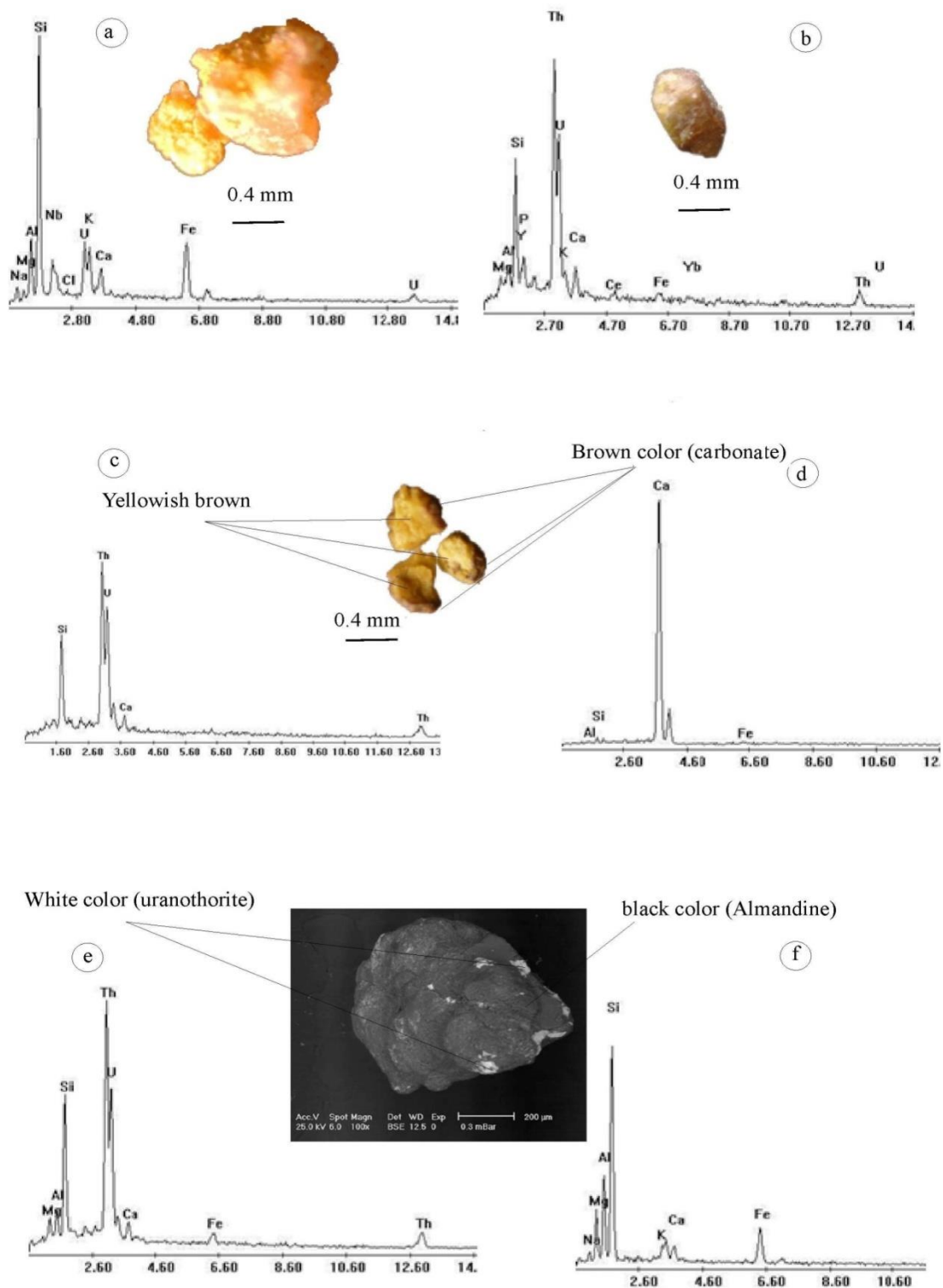


**Figure 4:** Optical microphotographs (R.L.) and ESEM image showing separated minerals and their EDX spectra: a. yellow patches of soddyite, b. yellowish brown metamict uranothorite, c & d. yellowish brown metamict uranothorite coated with carbonate and e & f. uranothorite and almandine garnet. R.L. = reflected light.

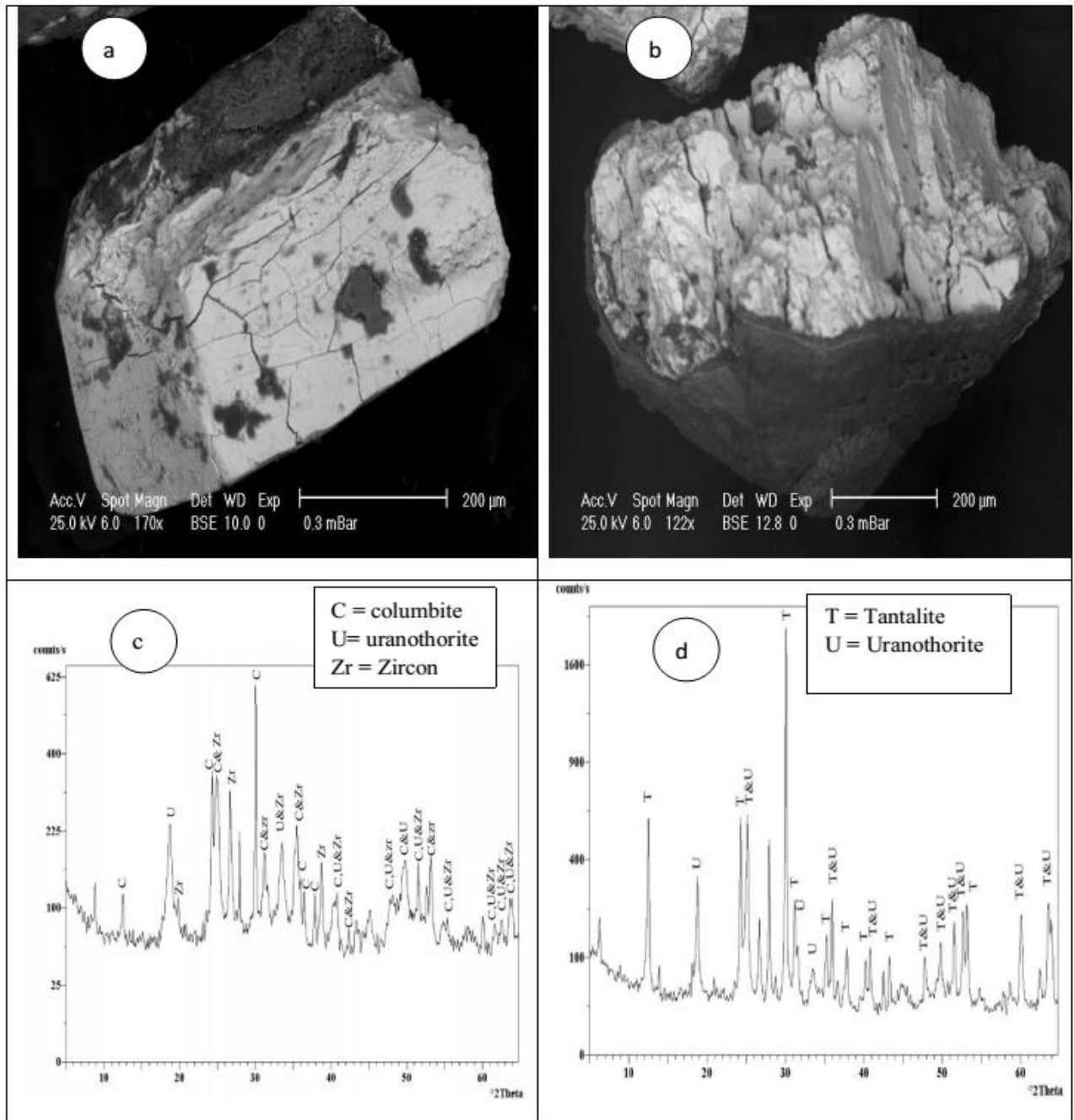


**Figure 5:** a. ESEM image of metamict uranorthorite (morphological variety 1), b. ESEM image of metamict uranorthorite (morphological variety 2) in studied leucogranite, c. XRD of assemblage crystals detected the presence of columbite, uranorthorite and zircon and d. XRD of assemblage crystals detected the presence of tantalite and uranorthorite in leucogranite.

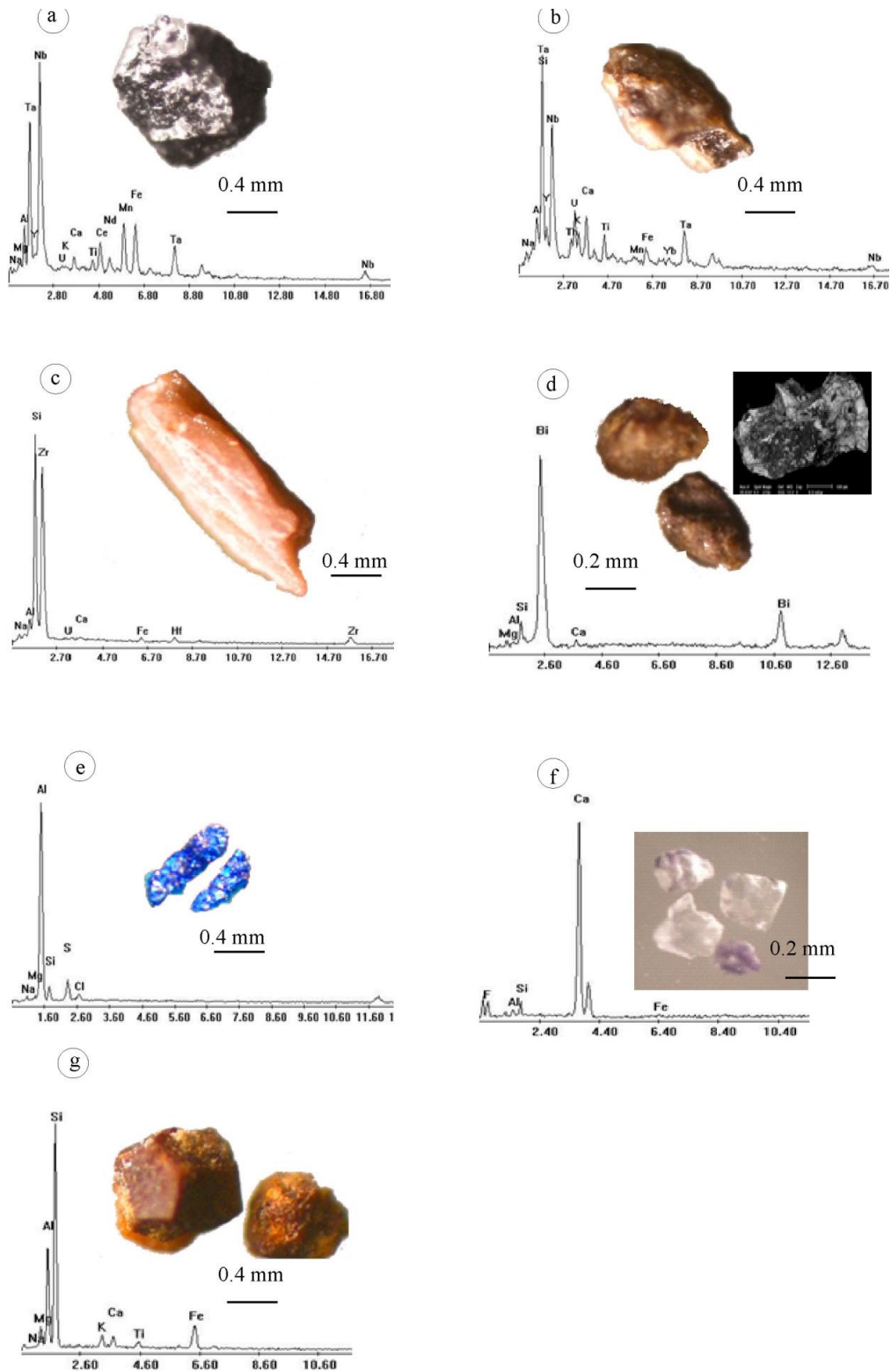


**Figure 6:** Optical (R.L.) and ESEM microphotographs show separated minerals and their EDX spectra: a. black columbite, b. brown tantalite, c. brown Hf- zircon, d. reddish bismuth, e. blue sapphire, f. colorless and violet fluorite and g. brown almandine garnet. R.L. = reflected light.

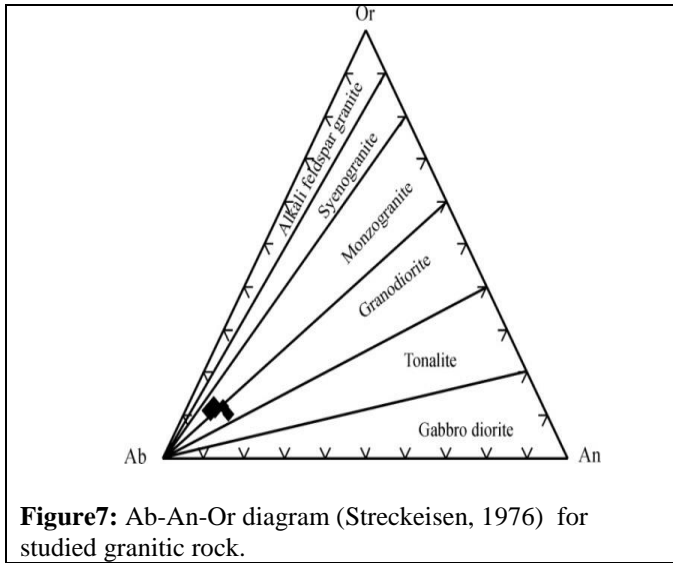


**Figure 7:** Ab-An-Or diagram (Streckeisen, 1976) for studied granitic rock.

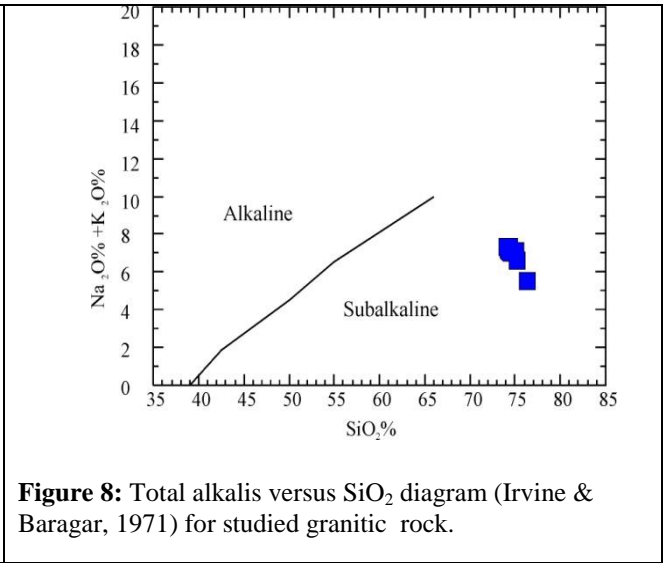


**Figure 8:** Total alkalis versus SiO<sub>2</sub> diagram (Irvine & Baragar, 1971) for studied granitic rock.

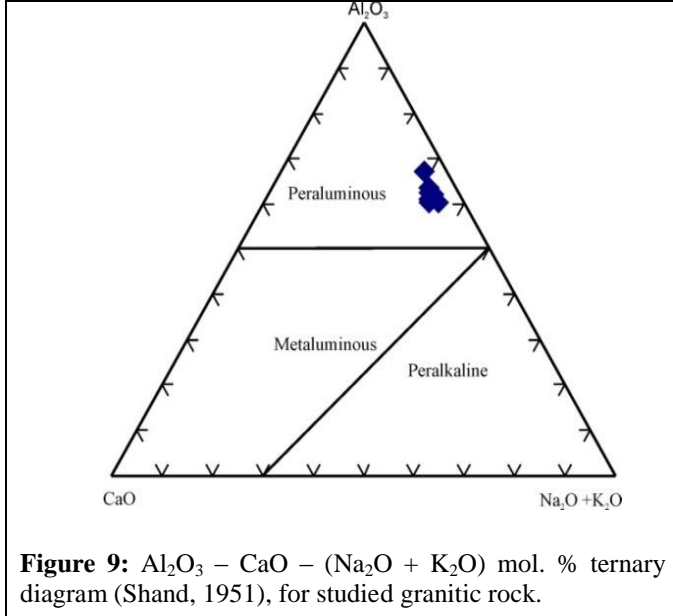


**Figure 9:** Al<sub>2</sub>O<sub>3</sub> - CaO - (Na<sub>2</sub>O + K<sub>2</sub>O) mol. % ternary diagram (Shand, 1951), for studied granitic rock.

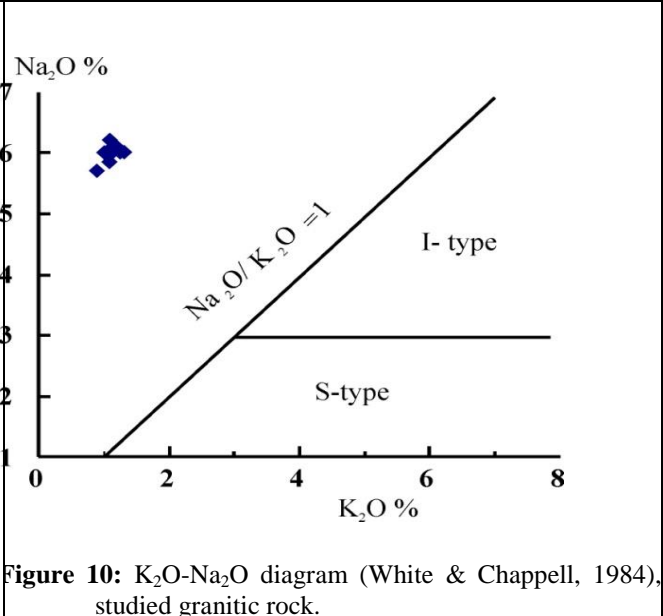


**Figure 10:** K<sub>2</sub>O-Na<sub>2</sub>O diagram (White & Chappell, 1984), studied granitic rock.

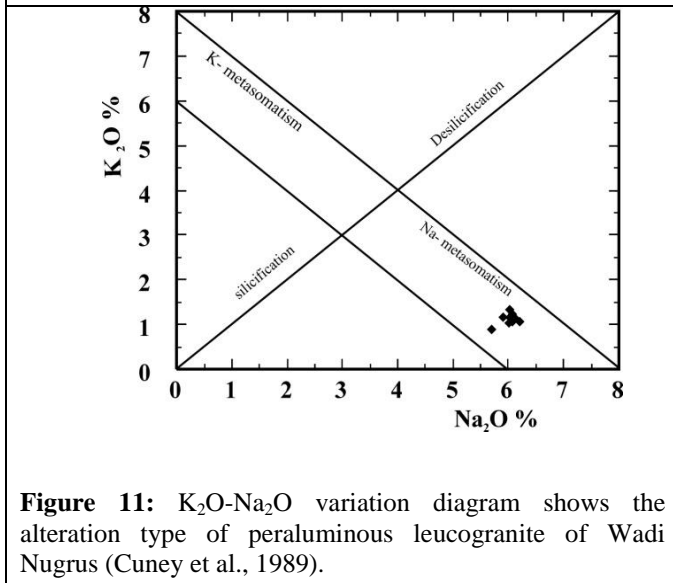


**Figure 11:** K<sub>2</sub>O-Na<sub>2</sub>O variation diagram shows the alteration type of peraluminous leucogranite of Wadi Nugrus (Cuney et al., 1989).

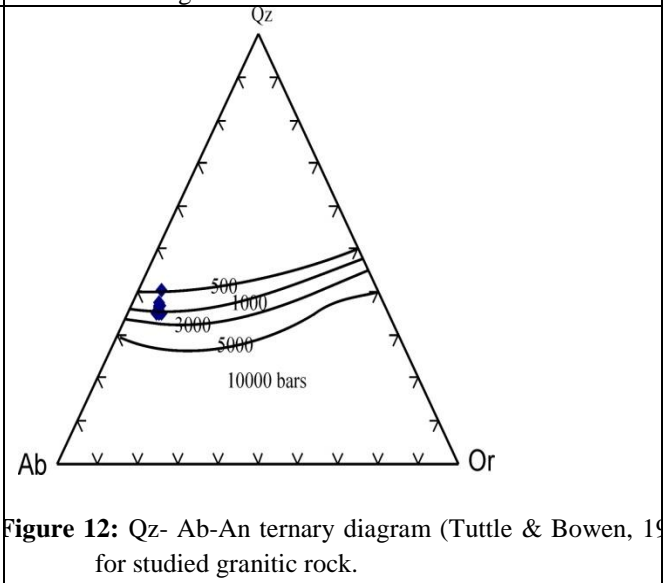


**Figure 12:** Qz- Ab-An ternary diagram (Tuttle & Bowen, 1958) for studied granitic rock.

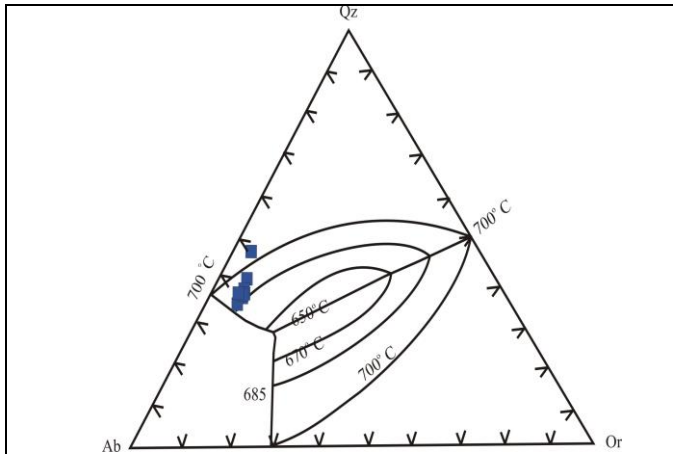


**Figure 13:** Qz- Ab-An ternary diagram (Tuttle & Bowen, 1958) for studied granitic rock.

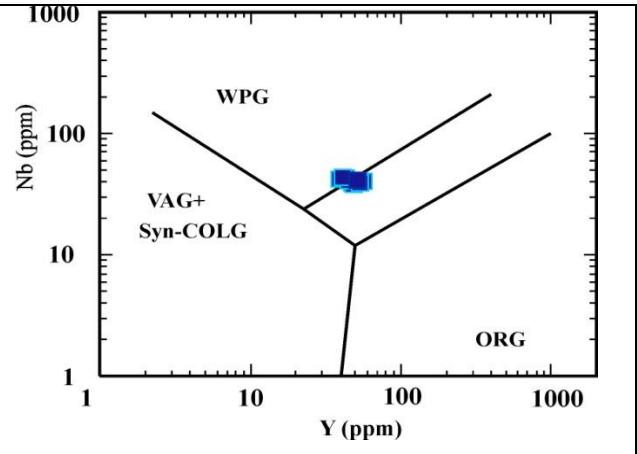


**Figure 14:** Nb-Y, according to Pearce et al. (1984), diagram studied granitic rock. Syn- COLG = Syncolli Granite, VAG = volcanic arc granite WPG = wi plate granite and ORG = oceanic ridge granite.

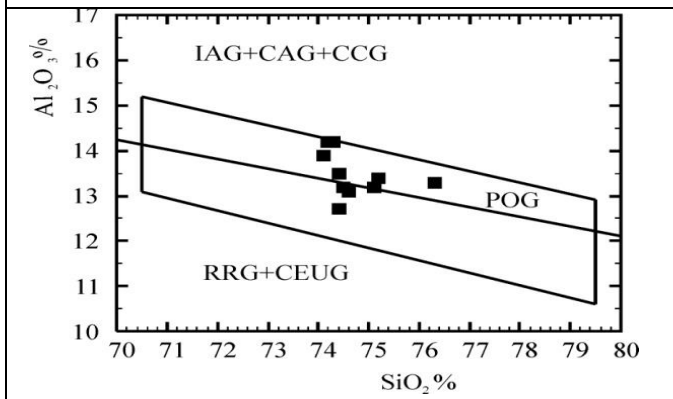


**Figure 15:** Al<sub>2</sub>O<sub>3</sub>-SiO<sub>2</sub> diagram (Maniar & Piccoli, 1989) studied granitic rock. Fields: IAG; island arc gran CAG; continental arc granites, CCG; continental colli granites, POG; post-orogenic granites, RRG; rift rel granites and CEUG; continental epirogenic u granites.

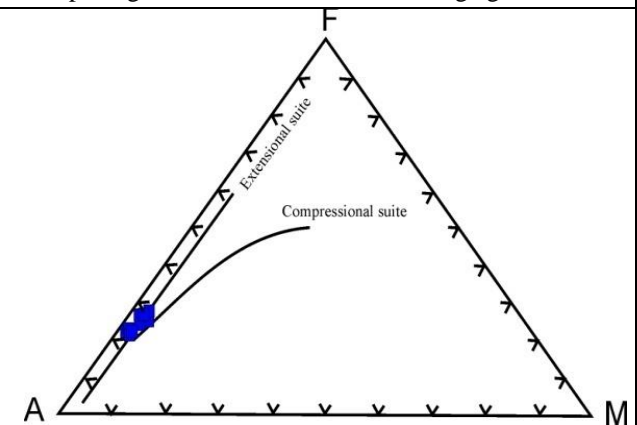


**Figure 16:** AFM ternary diagram (Petro et al., 1979) for the studied granitic rock.

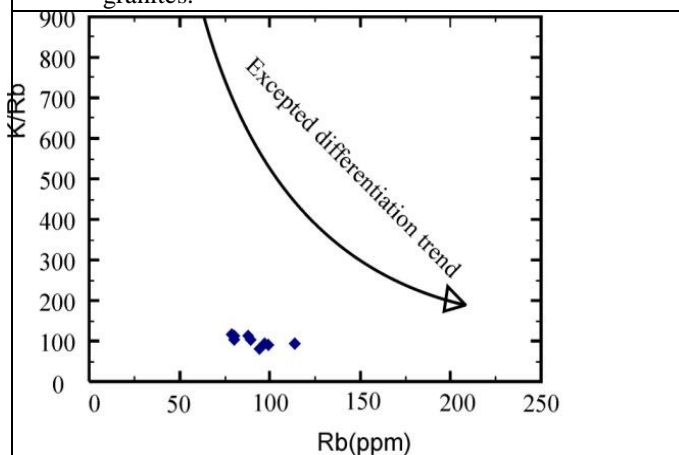


**Figure 17:** K/Rb - Rb binary diagram for studied granitic rock.

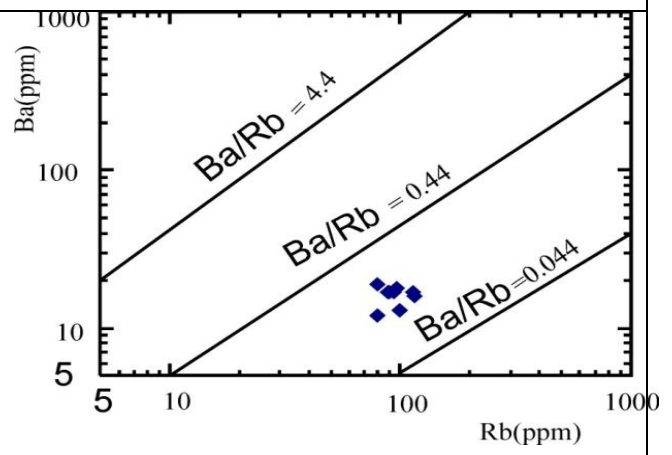


**Figure 18:** Ba - Rb binary diagram for studied granitic rock.

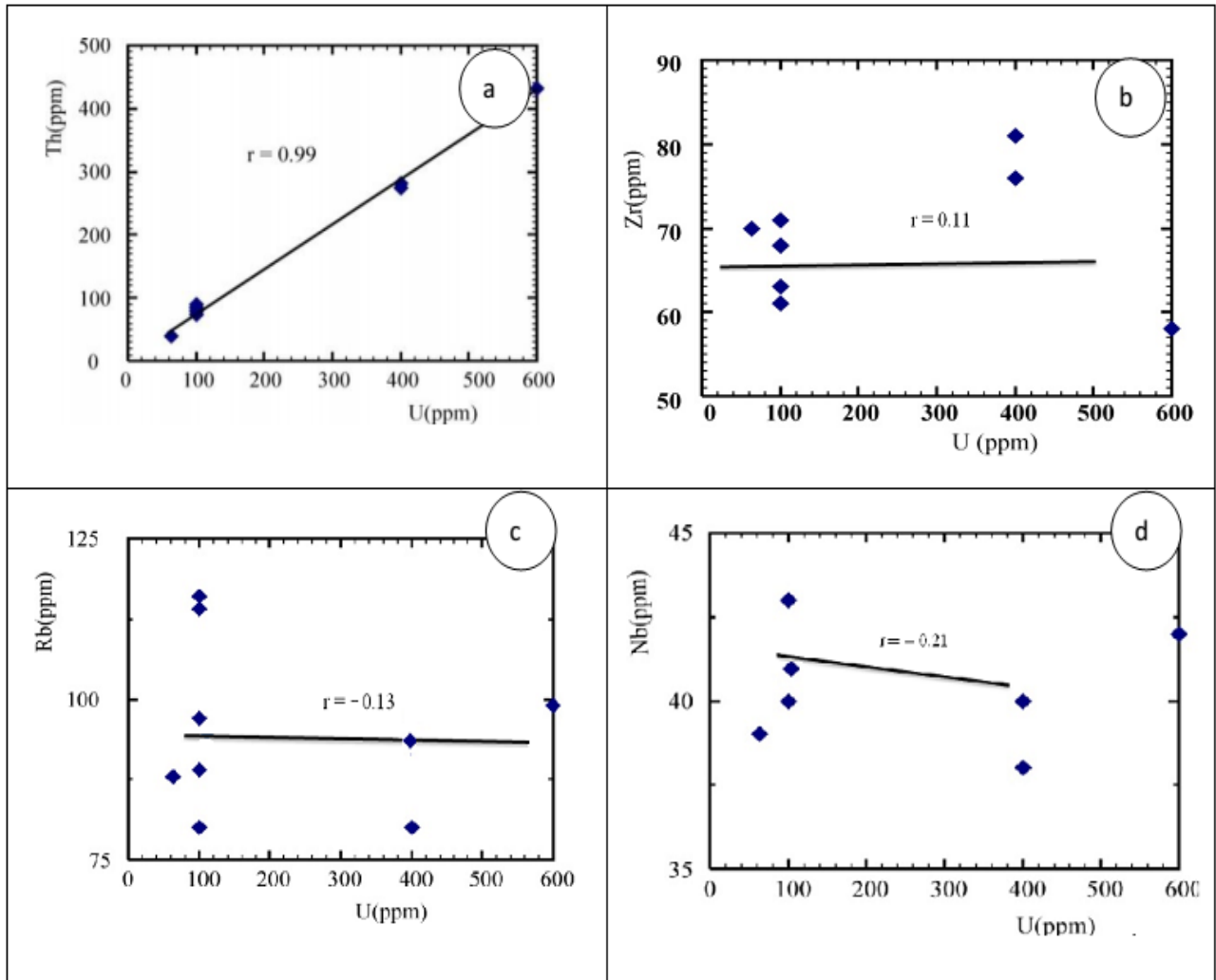


Figure 19: U versus trace elements (Th, Zr, Rb and Nb) for studied granitic rock.

**Tables:**

**Table 1:** major oxides (Wt %), trace elements (ppm), and norms (CIPM), differentiation index (D.I.) and geochemical ratios of MadinatNugrusperaluminousleucogranite.

Sample No.	1	2	3	4	5	6	7	8	9
<b>Major oxides (Wt %)</b>									
SiO <sub>2</sub>	74.6	75.2	74.2	74.3	75.1	74.4	74.5	74.4	74.1
Al <sub>2</sub> O <sub>3</sub>	13.1	13.4	14.2	13.4	13.2	13.5	13.2	12.7	12.9
TiO <sub>2</sub>	0.06	0.28	0.23	0.28	0.1	0.17	0.17	0.36	0.35
Fe <sub>2</sub> O <sub>3</sub>	2.6	1.9	2.7	2.2	2.1	2.1	2.8	2.3	2.5
MgO	0.36	0.24	0.2	0.3	0.2	0.2	0.3	0.4	0.6
CaO	1.4	1.1	1.3	1.5	1.1	1.1	1.2	1	1.1
P <sub>2</sub> O <sub>5</sub>	0.06	0.21	0.12	0.15	0.16	0.28	0.19	1.1	0.23
Na <sub>2</sub> O	5.9	5.7	6.1	6	6	6	6	6.2	6.1
K <sub>2</sub> O	1.1	0.9	1.1	1.3	1	1.1	1.1	1.1	1.2
L.O.I	0.3	0.4	0.3	0.3	0.3	0.2	0.07	0.1	0.4
<b>Total</b>	99.48	99.33	100.45	99.73	99.26	99.05	99.53	99.66	99.48
<b>Trace elements (ppm)</b>									
Cr	36	33	36	34	32	33	34	32	31
Ni	7	7	8	6	7	7	7	6	7
Cu	6	4	7	6	3	7	5	3	3
Zr	63	81	58	71	76	68	63	61	70
Zn	139	203	119	149	129	149	155	149	153
Rb	97	94	99	114	80	116	89	80	88
Y	40	56	39	51	49	46	43	41	48
Ba	18	17	13	17	19	16	17	12	17
Ga	25	24	24	24	23	25	25	25	25
Nb	43	40	42	41	38	40	43	43	39
Sr	u.d	2	u.d	u.d	2	u.d	u.d	u.d	2
Th	79	281	432	74	275	83	85	89	41
U	100	400	600	100	400	100	100	100	64
<b>CIPW</b>									
Qz	33.14	36.87	31.74	31.55	34.54	33.79	33.1	31.89	31.7
Or	6.26	5.38	5.38	6.5	7.73	5.98	6.58	6.58	6.54
Ab	50.28	48.7	51.48	51	51.24	51.3	50.98	52.63	52
An	6.05	4.27	7.74	5.81	4.57	3.86	4.87	3.58	4.15
C	.....	1.51	0.86	.....	0.59	1.1	0.36	...	0.10
Wo	0.25	.....	.....	0.33	.....	.....	.....	0.59	1.5
En	0.25	0.61	0.5	0.29	.....	0.51	0.75	0.51	.....
HY	0.69	.....	...	0.47	0.51	.....	.....	.....	.....
Hm	2.620.	1.92	2.7	2.21	2.12	1.62	2.82	2.31	2.52
Ap	0.13	0.46	0.26	0.33	0.35	0.62	0.42	.....	0.51
D.I.	89.68	90.95	89.28	90.28	91.76	91.67	90.6	91.1	90.89
<b>Geochemical ratios</b>									
Na <sub>2</sub> O/K <sub>2</sub> O	5.3	6.3	5.5	4.6	6	5.4	5.5	5.6	5
K/Rb	93.81	79.79	91.92	95.61	103.75	78.44	102.24	113.75	114.77
Ba/Rb	0.186	0.18	0.13	0.14	0.24	0.14	0.191	0.15	0.193
K/Ba	505.55	441.17	700	441.17	436.84	568.75	535.29	758.33	594.17
Th/ U	0.79	0.7	0.72	0.74	0.69	0.83	0.85	0.89	0.63

u.d = under detection limit

**Table 2:** Comparison between the concentration of elements Nb, Ta, Mn, Fe, Ce, Al and Y (in wt%) from the margin and the core of columbite crystal obtained by EDX analysis.

element	margin	core
Nb%	49.21	59.17
Ta%	18.72	18.16
Mn%	6.95	6.22
Fe%	7.03	12.08
Ce%	8.8	0.37
Al%	3.28	0.5
Y%	1.31	0.87

**Table 3:** Average major contents of elements in the studied peraluminous granite compared with similar averages in some Egyptian and World granites.

Major Oxides	1	2	3	4	5	6
SiO <sub>2</sub>	74.53	74.80	70.1	69.89	71.3	73.2
Al <sub>2</sub> O <sub>3</sub>	13.28	12.80	14.1	12.26	14.3	13.7
TiO <sub>2</sub>	0.22	0.15	0.47	0.25	0.31	0.22
Fe <sub>2</sub> O <sub>3</sub>	2.35	1.09	2.84	3.17	1.2	1.1
FeO	n. d.	n. d.	n. d.	1.54	1.64	0.97
MnO	n. d.	n. d.	n. d.	0.11	0.05	0.05
MgO	0.31	0.11	0.64	2.45	0.71	0.46
CaO	1.2	0.57	1.71	2.49	1.84	1.19
Na <sub>2</sub> O	6	3.99	4.57	4.16	3.68	3.84
K <sub>2</sub> O	1.1	4.62	3.64	1.45	4.1	4.28
P <sub>2</sub> O <sub>5</sub>	0.27	0.05	0.15	0.12	0.12	0.11

n. d. = not detected.

1 = Granites of WadiNugrus area (present work)

2 = Group II younger granites of Eastern Desert (Greenberg, 1981).

3 = Group III younger granites of Eastern Desert (Greenberg, 1981).

4 = Two-mica granite of G. El Sella area, South Eastern Desert (Ibrahim et al., 2003).

5 = Average of world granites (Le maitre, 1976).

6 = Average of Egyptian granites (Aly&Moustafa, 1984).